



## The Cells and Circuitry for Itch Responses in Mice

Santosh K. Mishra and Mark A. Hoon

*Science* **340**, 968 (2013);

DOI: 10.1126/science.1233765

*This copy is for your personal, non-commercial use only.*

If you wish to distribute this article to others, you can order high-quality copies for your colleagues, clients, or customers by [clicking here](#).

Permission to republish or repurpose articles or portions of articles can be obtained by following the guidelines [here](#).

**The following resources related to this article are available online at [www.sciencemag.org](http://www.sciencemag.org) (this information is current as of May 25, 2013 ):**

**Updated information and services**, including high-resolution figures, can be found in the online version of this article at:

<http://www.sciencemag.org/content/340/6135/968.full.html>

**Supporting Online Material** can be found at:

<http://www.sciencemag.org/content/suppl/2013/05/23/340.6135.968.DC1.html>

This article **cites 25 articles**, 10 of which can be accessed free:

<http://www.sciencemag.org/content/340/6135/968.full.html#ref-list-1>

This article appears in the following **subject collections**:

Neuroscience

<http://www.sciencemag.org/cgi/collection/neuroscience>

to the content of substituted Fe in  $Mn_3O_4$ . The potential of  $Mn_{3-x}Fe_xO_4$  as a function of the Fe content was investigated through density functional theory calculations, which indicated that a solid solution of  $Mn_{3-x}Fe_xO_4$  can occur between  $Mn_3O_4$  and  $Fe_3O_4$  (fig. S20) and that their average reaction voltages are proportional to the amount of the  $Fe_3O_4$  component from 0.400 to 0.818 V at  $0 \leq x \leq 3$  (table S2) (20). Our results suggest that the potentials of multicomponent spinel electrode materials can be easily tuned by galvanic replacement reaction and subsequent thermal treatment.

Figure 3D shows cycle performances of hollow  $Mn_{3-x}Fe_xO_4$  NCs.  $Mn_{1.1}Fe_{1.9}O_4$  exhibited first discharge and charge capacities of 1339 and 984 mAh  $g^{-1}$ , respectively.  $Mn_{1.1}Fe_{1.9}O_4$  exhibited a high reversible capacity of  $\sim 1000$  mAh  $g^{-1}$  with almost no fading up to 50 cycles. The reversible capacities and cyclic stabilities of  $Mn_{2.0}Fe_{1.0}O_4$  and  $Mn_{1.5}Fe_{1.5}O_4$  were comparable to those of  $Mn_{1.1}Fe_{1.9}O_4$ . Most of the samples showed higher specific capacities and better cyclic stabilities than those of carbon-coated solid  $Mn_{0.8}Fe_{2.2}O_4$  NCs (fig. S21) (20). These good cyclic stabilities can be attributed to their hollow structure, which provides extra free space for alleviating the structural strain caused by the large volume change (26, 27) and additional sites for lithium ion storage (28).  $Mn_{0.6}Fe_{2.4}O_4$  and  $Mn_{0.3}Fe_{2.7}O_4$ , which are close to  $Fe_3O_4$ , showed less cyclic stability than the other samples, indicating that multi-metallic composition contributes to the enhanced cyclic stabilities (29). Furthermore,  $Mn_{1.1}Fe_{1.9}O_4$  exhibited the highest rate capability (fig. S22)

(20), which is due to the improvement in its electronic conductivity resulting from the mixed valency of the multicomponent  $Mn_{3-x}Fe_xO_4$  (30).

#### References and Notes

1. Y. Sun, Y. Xia, *Science* **298**, 2176 (2002).
2. G. S. Métraux, Y. C. Cao, R. Jin, C. A. Mirkin, *Nano Lett.* **3**, 519 (2003).
3. Y. Sun, Y. Xia, *J. Am. Chem. Soc.* **126**, 3892 (2004).
4. S. E. Skrabalak *et al.*, *Acc. Chem. Res.* **41**, 1587 (2008).
5. J. E. Macdonald, M. Bar Sadan, L. Houben, I. Popov, U. Banin, *Nat. Mater.* **9**, 810 (2010).
6. Z. Peng, H. You, J. Wu, H. Yang, *Nano Lett.* **10**, 1492 (2010).
7. E. González, J. Arbiol, V. F. Puntes, *Science* **334**, 1377 (2011).
8. F. Xiao, B. Yoo, K. H. Lee, N. V. Myung, *J. Am. Chem. Soc.* **129**, 10068 (2007).
9. Z. Wang, L. Zhou, X. W. (David) Lou, *Adv. Mater.* **24**, 1903 (2012).
10. Y. Piao *et al.*, *Nat. Mater.* **7**, 242 (2008).
11. Y. Yin *et al.*, *Science* **304**, 711 (2004).
12. D. H. Son, S. M. Hughes, Y. Yin, A. P. Alivisatos, *Science* **306**, 1009 (2004).
13. J. Park, H. Zheng, Y. W. Jun, A. P. Alivisatos, *J. Am. Chem. Soc.* **131**, 13943 (2009).
14. S. Peng, S. Sun, *Angew. Chem. Int. Ed.* **46**, 4155 (2007).
15. A. Cabot *et al.*, *J. Am. Chem. Soc.* **129**, 10358 (2007).
16. A. Cabot, M. Ibañez, P. Guardia, A. P. Alivisatos, *J. Am. Chem. Soc.* **131**, 11326 (2009).
17. Q. Zhang, W. Wang, J. Goebel, Y. Yin, *Nano Today* **4**, 494 (2009).
18. G. D. Moon *et al.*, *Nano Today* **6**, 186 (2011).
19. T. Yu *et al.*, *Chem. Mater.* **21**, 2272 (2009).
20. Materials and methods are available as supplementary materials on Science Online.
21. J. E. Villinski, P. A. O'Day, T. L. Corley, M. H. Conklin, *Environ. Sci. Technol.* **35**, 1157 (2001).
22. J.-S. Kang *et al.*, *Phys. Rev. B* **77**, 035121 (2008).

23. X. Wu *et al.*, *Angew. Chem. Int. Ed.* **51**, 3211 (2012).
24. V. B. Fetisov, G. A. Kozhina, A. N. Ermakov, A. V. Fetisov, E. G. Miroschnikova, *J. Solid State Electrochem.* **11**, 1205 (2007).
25. H. Wang *et al.*, *J. Am. Chem. Soc.* **132**, 13978 (2010).
26. H. S. Kim, Y. Piao, S. H. Kang, T. Hyeon, Y.-E. Sung, *Electrochem. Commun.* **12**, 382 (2010).
27. C. K. Chan *et al.*, *Nat. Nanotechnol.* **3**, 31 (2008).
28. B. Koo *et al.*, *Nano Lett.* **12**, 2429 (2012).
29. M. Li *et al.*, *Chem. Commun.* **48**, 410 (2012).
30. J. Kim, S.-W. Kim, H. Gwon, W.-S. Yoon, K. Kang, *Electrochim. Acta* **54**, 5914 (2009).

**Acknowledgments:** We acknowledge financial support by the Research Center Program of the IBS in Korea (T.H. and Y.-E.S.); the WCU (R31-10013) Program of the National Research Foundation (NRF) of Korea (T.H., N.P., and Y.-E.S.); Portuguese Fundação para a Ciência e a Tecnologia projects (PTDC/CTM/100468/2008 and REDE/1509/RME/2005) for TEM work (M.-G.W. and N.P.); a Human Resources Development of the Korea Institute of Energy Technology Evaluation and Planning grant funded by the Korea government Ministry of Trade, Industry and Energy (20124010203320) (K.K. and D.-H.S.); and National Creative Initiative (2009-0081576), WCU (R31-2009-000-10059), and Max Plank POSTECH/KOREA Research Initiative (2011-0031558) programs through the NRF of Korea (K.-T.K. and J.-H.P.). The Pohang Accelerator Laboratory is supported by POSTECH and the Ministry of Science, ICT and Future Planning.

#### Supplementary Materials

www.sciencemag.org/cgi/content/full/340/6135/964/DC1  
Materials and Methods  
Supplementary Text  
Figs. S1 to S22  
Tables S1 and S2  
References (31–43)

3 January 2013; accepted 15 April 2013  
10.1126/science.1234751

## The Cells and Circuitry for Itch Responses in Mice

Santosh K. Mishra and Mark A. Hoon\*

Itch is triggered by somatosensory neurons expressing the ion channel TRPV1 (transient receptor potential cation channel subfamily V member 1), but the mechanisms underlying this nociceptive response remain poorly understood. Here, we show that the neuropeptide natriuretic polypeptide b (Nppb) is expressed in a subset of TRPV1 neurons and found that Nppb<sup>-/-</sup> mice selectively lose almost all behavioral responses to itch-inducing agents. Nppb triggered potent scratching when injected intrathecally in wild-type and Nppb<sup>-/-</sup> mice, showing that this neuropeptide evokes itch when released from somatosensory neurons. Itch responses were blocked by toxin-mediated ablation of Nppb-receptor-expressing cells, but a second neuropeptide, gastrin-releasing peptide, still induced strong responses in the toxin-treated animals. Thus, our results define the primary pruriceptive neurons, characterize Nppb as an itch-selective neuropeptide, and reveal the next two stages of this dedicated neuronal pathway.

Pruritic responses are triggered by somatosensory neurons, with several itch-inducing agents acting through pathways involving the ion channel TRPV1 (transient receptor po-

tential cation channel subfamily V member 1) (1, 2) and the effector enzyme PLCβ3 (3). Recently, agonist-induced silencing of TRPV1-expressing neurons was shown to result in a profound loss of all itch responses (2) but also affects thermosensation and pain (4). In contrast, a much more specific loss of pruriception was observed in mice lacking the gastrin-releasing peptide (GRP) receptor (5) and in animals in which the spinal interneurons expressing this receptor had been

specifically targeted with a GRP-conjugated toxin (GRP-saporin) (6). Thus, it was hypothesized that GRP is the neurotransmitter that initiates a labeled line for itch (5, 6).

Previously, we generated mice that had lost all TRPV1-lineage neurons (7). These mice have major pruritic deficits (Fig. 1A) as well as a complete loss of thermosensory input (7), which is in keeping with previous reports that used capsaicin-induced lesions (2, 4). To identify candidate molecules that might mediate itch signaling, we used a differential microarray-based screen that identified many TRPV1-enriched transcripts (table S1). Among these, natriuretic polypeptide b (Nppb) is prominently expressed in a small subset of dorsal root ganglia (DRG) neurons but is dramatically decreased in sensory ganglia from TRPV1-DTA animals (Fig. 1B). Double-label in situ hybridization (ISH) explicitly demonstrates that all Nppb-expressing neurons contain TRPV1 (Fig. 1C) and PLCβ3 (Fig. 1D), which are critically required for histamine-induced scratching in mice (2, 3). Moreover, double labeling (Fig. 1, E and F) shows almost complete overlap between the expression of Nppb and two Mas-related G protein-coupled receptors that have recently been shown to detect specific pruritogens (8–10).

We generated Nppb<sup>-/-</sup> animals (Fig. 2A) and showed that these mutants displayed no detect-

Molecular Genetics Unit, Laboratory of Sensory Biology, National Institute of Dental and Craniofacial Research (NIDCR), NIH, Building 49, Room 1A16, 49 Convent Drive, Bethesda, MD 20892, USA.

\*Corresponding author. E-mail: mark.hoon@nih.gov

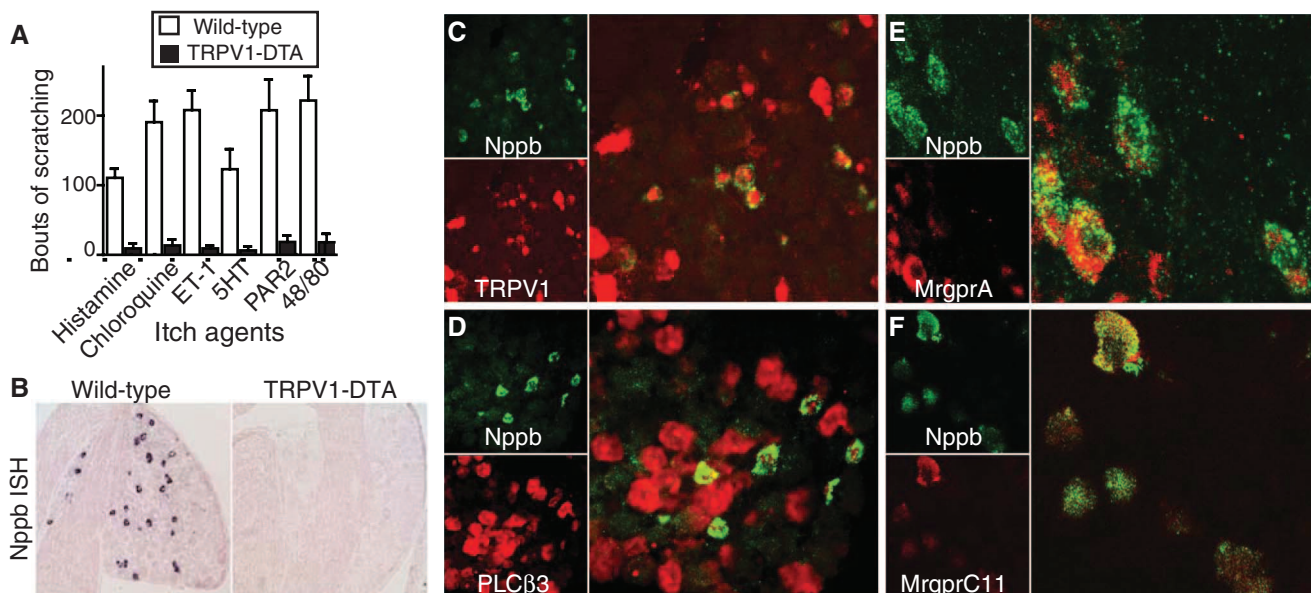


**Fig. 1. Nppb is always coexpressed with itch-related signaling molecules TRPV1 and PLCβ3.** (A) TRPV1-DTA mice exhibit dramatically reduced scratch responses after intradermal injection of pruritic agents; histamine (100 μg in 10 μl); chloroquine (100 μg); endothelin 1 (1 μM); methyl-serotonin (30 μg); PAR2 agonist SLIGRL-NH<sub>2</sub> (100 μg); and compound 48/80 (100 μg). Itch-inducing substances were injected intradermally into the shoulder of mice, and numbers of scratching bouts were assessed over 30 min; data are mean ± SEM (*n* ≥ 7 animals) normalized to wild-type litter controls. (B) ISH of sections through DRG illustrating loss of Nppb-expression in TRPV1-DTA animals. Quantitation of Nppb-expressing neurons revealed that 7 ± 0.6% of NeuN-positive C4 DRG neurons express the neuropeptide in wild-type mice

(*n* = 3 animals). (C) Double-label ISH of DRG demonstrates that Nppb (green) and TRPV1 (red) are coexpressed in the same sensory neurons; only a subset of TRPV1-expressing neurons contain Nppb. (D) All Nppb-positive neurons also express PLCβ3 (red), but many PLCβ3 neurons are Nppb-negative. (E) Double-label ISH also shows that Nppb-positive neurons (green) all express MrgprA receptors (including MrgprA3, the receptor for chloroquine; red), with more than 70% of MrgprA-expressing neurons also containing the neuropeptide. (F) Double-label immunostaining demonstrates complete overlap between expression of MrgprC11 (red), the receptor for the pruritogen SLIGRL-NH<sub>2</sub>, and Nppb (green) in somatosensory neurons. Additional characterization of neurons expressing Nppb is available in fig. S2.

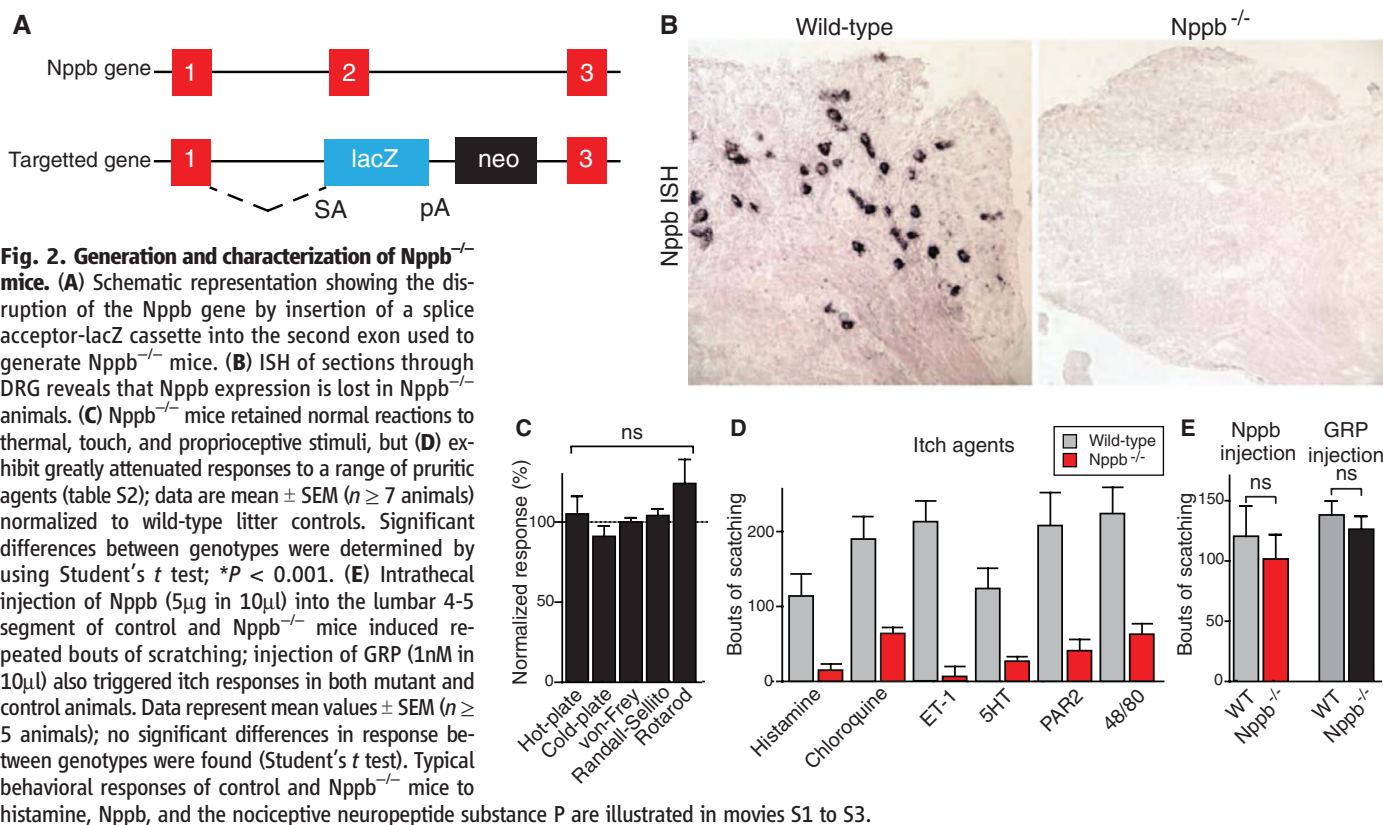


**Fig. 2. Generation and characterization of Nppb<sup>-/-</sup> mice.** (A) Schematic representation showing the disruption of the Nppb gene by insertion of a splice acceptor-lacZ cassette into the second exon used to generate Nppb<sup>-/-</sup> mice. (B) ISH of sections through DRG reveals that Nppb expression is lost in Nppb<sup>-/-</sup> animals. (C) Nppb<sup>-/-</sup> mice retained normal reactions to thermal, touch, and proprioceptive stimuli, but (D) exhibit greatly attenuated responses to a range of pruritic agents (table S2); data are mean ± SEM (*n* ≥ 7 animals) normalized to wild-type litter controls. Significant differences between genotypes were determined by using Student's *t* test; \**P* < 0.001. (E) Intrathecal injection of Nppb (5 μg in 10 μl) into the lumbar 4-5 segment of control and Nppb<sup>-/-</sup> mice induced repeated bouts of scratching; injection of GRP (1 nM in 10 μl) also triggered itch responses in both mutant and control animals. Data represent mean values ± SEM (*n* ≥ 5 animals); no significant differences in response between genotypes were found (Student's *t* test). Typical behavioral responses of control and Nppb<sup>-/-</sup> mice to histamine, Nppb, and the nociceptive neuropeptide substance P are illustrated in movies S1 to S3.

able expression of Nppb (Fig. 2B). The mice were healthy, had normal numbers of nociceptive, touch, and proprioceptive neurons, and the distribution and number of dorsal horn interneurons was unaffected by gene disruption (fig. S1). Nppb<sup>-/-</sup> mice retained normal responses to thermal, nociceptive, touch, and proprioceptive stimulation when tested with standard assays (Fig. 2C). We performed intradermal injections and recorded numbers of scratching bouts for substances that directly activate pruriceptors and with compound 48/80 that causes itch via an indirect route (11). All of these agents (table S2) reliably triggered multiple bouts of scratching in control animals (Fig. 2D, gray bars), but Nppb<sup>-/-</sup> mice were almost completely insensitive to the full range of pruritic substances tested (Fig. 2D, red bars).

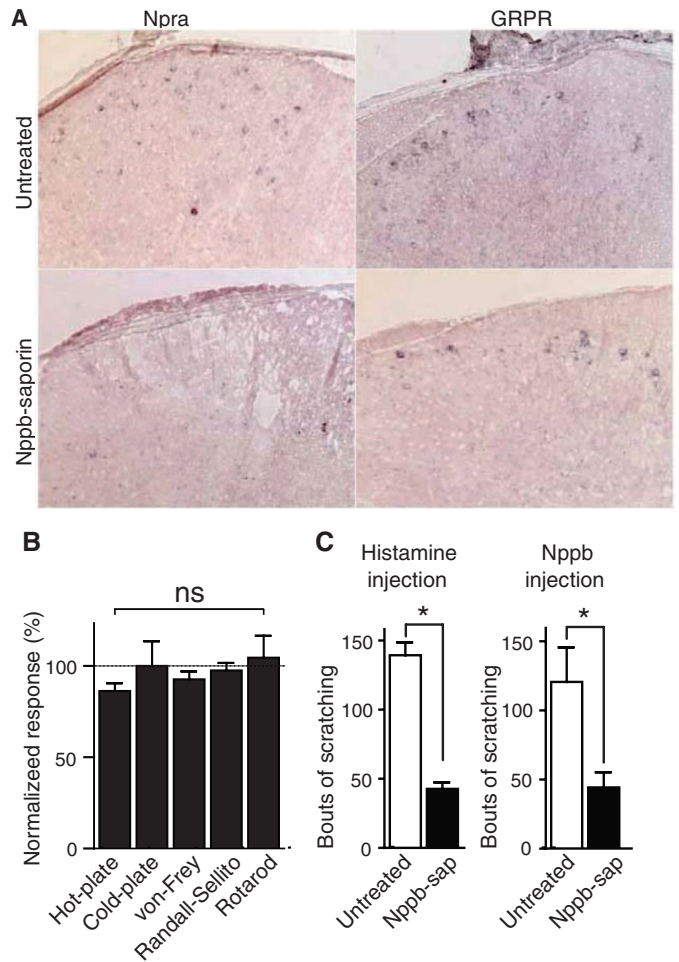
How does Nppb induce this stereotyped scratch response? We reasoned that because this peptide is prominently expressed in somatosensory neurons, the most plausible explanation for its role would be if it acted as a specific itch-related neuromodulator (or neurotransmitter) in the spinal cord. Indeed, intrathecal injection of Nppb induced profound scratching behavior in wild-type animals (Fig. 2E, gray bar), demonstrating that spinal-Nppb is sufficient to induce itch even without activation of the peripheral neurons that express it. Intrathecal injection of Nppb into Nppb<sup>-/-</sup> mice also led to an equivalent phenotype (Fig. 2E, red bar). Loss of Nppb in sensory afferents was thus responsible for the prurceptive deficits seen in mutant mice. Therefore, we suggest that Nppb-expression delineates the subset of somatosensory neurons that detect pruritic agents and that central release of Nppb from these neurons is necessary for the itch response.

Because Nppb is responsible for transmitting the peripheral signals that trigger pruritic responses, its receptor Npra (12) should be expressed at the site of afferent fiber synaptic connections in the spinal dorsal horn and mark the secondary neurons in the itch-response circuit. Therefore, we used ISH to localize Npra expression in the dorsal horn and found that it is indeed expressed in a limited subset of neurons (most likely interneurons), primarily in the outer layer—lamina I (Fig. 3A, left)—corresponding to the terminal field of TRPV1-expressing sensory neurons (13).

To examine whether the Npra neurons in the spinal cord function in the itch circuit and whether they are selectively required for pruritogen-induced scratching (rather than other somatosensory responses), we used a targeted-toxin cell-ablation strategy (14). We injected a Nppb-saporin conjugate intrathecally into wild-type mice so as to target their Npra-expressing cells and assessed the effectiveness, specificity, and behavioral consequences of administering this toxin. Approximately 70% of Npra-positive neurons were eliminated after administration of toxin (Fig. 3A and fig. S3). This targeting was highly selective, with neither cells expressing the GRP-receptor nor other dorsal horn interneurons affected by Nppb-saporin treat-

### Fig. 3. Selective ablation of Npra receptor neurons in the spinal cord impairs pruriception.

(A) Expression of Npra in the dorsal spinal cord was assessed by using ISH. In normal mice (top), a subset of interneurons in the outer layer express Npra; however, after intrathecal administration of Nppb-saporin (bottom), few Npra neurons remained. In contrast, the number of GRP-receptor-positive cells (right) were unaffected by Nppb-saporin. (B) Nppb-saporin-treated mice retain normal reactions to thermal, touch, and proprioceptive stimuli, but (C) exhibit greatly attenuated responses to intradermal injection of histamine (100  $\mu$ g in 10  $\mu$ l) or intrathecal administration of Nppb. Data represent means normalized against untreated controls  $\pm$  SEM ( $n \geq 5$  animals). Significant differences between genotypes were determined by using Student's *t* test; \* $P < 0.01$ .



ment (Fig. 3A and fig. S3). Toxin-injected mice displayed normal responses to thermal, touch, and painful stimulation (Fig. 3B). However, we observed a dramatic reduction in scratching evoked by histamine (Fig. 3C), indicating that these neurons are required for itch responses but not for other somatosensory pathways.

How do these findings fit with current models of itch behavior? The GRP-receptor has been shown to be a key element in the pruritic pathway (5, 6), with the suggestion that GRP might be the primary neurotransmitter for itch. However, this view has also been questioned (11, 15). We were unable to detect more than trace quantities of GRP expression in the DRG using a sensitive quantitative polymerase chain reaction (PCR) assay (Fig. 4A). Similarly, somatosensory neurons from GRP-reporter mice—Tg(GRP-EGFP)—were negative for enhanced green fluorescent protein (EGFP) expression (fig. S4A). In contrast, ISH for GRP and analysis of EGFP expression in the GRP-reporter mice revealed that this neuropeptide is present in a population of neurons in the dorsal horn (Fig. 4B and fig. S4A), as reported previously (15, 16). Therefore, we concluded that GRP cannot act at the level of pruriception but must function downstream of Nppb and so applied three complementary functional strategies

to substantiate this hypothesis and dissect the itch-response circuit.

First, we demonstrated that GRP-induced scratching was unaltered either by knocking out Nppb (Fig. 2E) or by the ablation of Npra-expressing neurons (Fig. 4D). Second, we showed that pharmacological inhibition of the GRP-receptor not only attenuated behavioral responses to the pruritic agent histamine or GRP injection (fig. S4B) but also inhibited scratching after intrathecal administration of Nppb (Fig. 4E). Last, we tested mice with selective ablation of GRP-receptor-expressing neurons and again found significantly reduced itch responses to Nppb (Fig. 4E). These data place GRP downstream of Nppb in the itch response circuit and suggest that the secondary pruriceptors are targets for one neuropeptide, Nppb, and in turn signal through a second peptide, GRP. Just as this model predicts, all Npra-expressing neurons in the dorsal horn contain GRP (Fig. 4F), and Nppb-saporin treatment significantly reduces the number of GRP-expressing cells (Fig. 4B, right).

Our results molecularly characterize the first three stations of an itch response pathway in mice (Fig. 4G), demonstrate that Nppb marks the primary sensory neurons, and show that this peptide is both necessary and sufficient for transmission

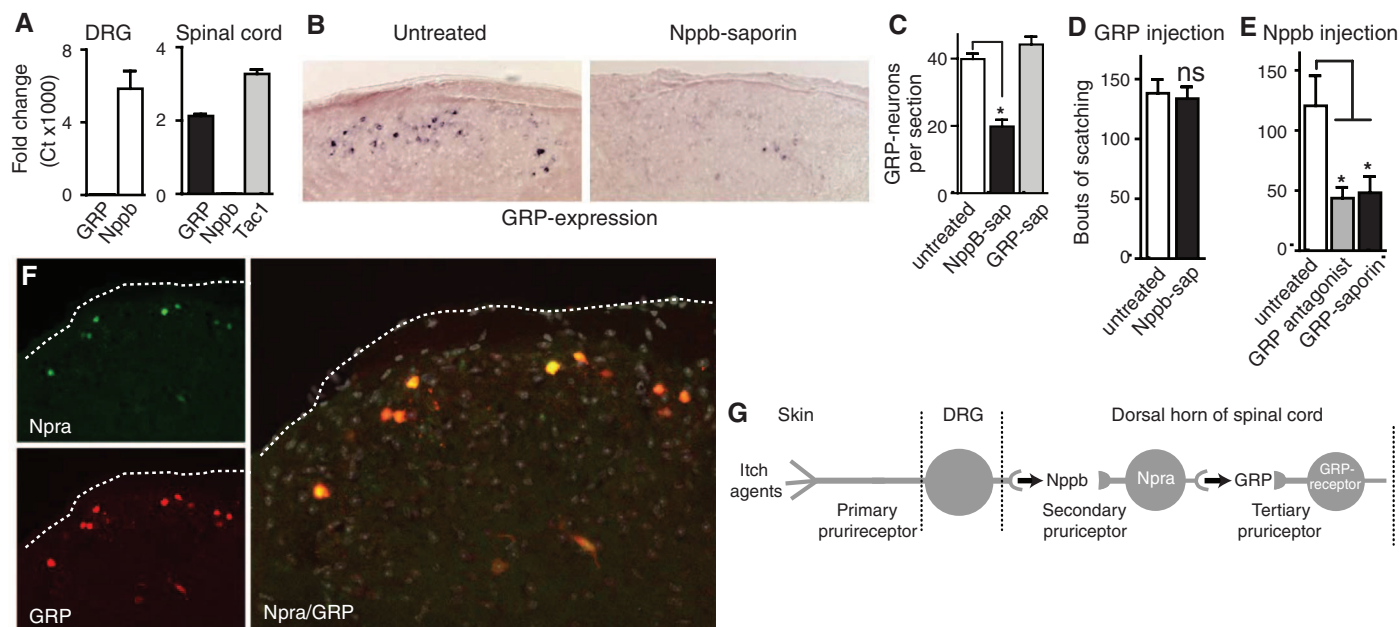


**Fig. 4. GRP acts directly downstream of Nppb in the rodent prurceptive circuit.** (A) Quantitative PCR was used to quantitate expression of GRP and Nppb relative to glyceraldehyde-3-phosphate dehydrogenase (GAPDH) in the DRG and spinal cord. GRP is robustly expressed in the spinal cord (at a level comparable with Tac1) but is almost undetectable in the DRG. Nppb is prominently expressed in DRG but is not present in the spinal cord. Data represent mean  $\pm$  SEM for triplicate cDNA preparations each analyzed in two separate PCR reactions. (B) ISH was used to analyze GRP expression in the dorsal horn of normal (left) and Nppb-saporin treated mice (right); many GRP-expressing interneurons are lost on ablation of Npra-expressing cells. (C) A significant number of GRP neurons was eliminated after Nppb-saporin (Nppb-sap) treatment. GRP-saporin (GRP-sap), which targets GRP-receptor neurons, has no effect on the number of GRP interneurons; data represent mean  $\pm$  SEM

( $n \geq 4$  animals). Significant differences between groups were determined by using Student's *t* test; \* $P < 0.001$ . (D) Ablation of Npra neurons had no effect on intrathecally administered GRP-induced scratch responses. (E) Scratching induced by means of lumbar injection of Nppb was strongly attenuated by pretreatment with a selective GRP antagonist or by the ablation of GRPR-expressing neurons with GRP-saporin. Data in (D) and (E) are mean  $\pm$  SEM ( $n \geq 6$  animals); \* $P < 0.001$  (Student's *t* test). (F) Double-label immunohistochemistry was used to localize interneurons expressing Npra (green) and GRP-driven EGFP (red) in sections through the dorsal horn of Tg(GRP-EGFP) mice. (Left) Typical individual staining patterns. (Right) Merged Npra and GRP images, with the cell nuclei counterstained with DAPI (gray); the outline of the dorsal horn is dotted. (G) Model of the first three stages of the prurceptive circuit, with the critical neuropeptide used at each stage indicated.

of peripheral signals that induce stereotypic itch responses. Unlike previously characterized receptors (8, 9) and signaling molecules (1–3) that affect the detection of particular itch-inducing agents, Nppb is necessary for responses to a wide range of pruritogens (compounds classed as inducing histamine- and nonhistamine-related itch) (table S2). Our data also refine the role GRP and GRP-receptor cells play in the itch-response pathway by placing them at later stages than had been hypothesized previously (5, 6). Many questions about itch remain unanswered, including its close relationship to sensing pain (17) and its slow kinetics and long duration, as well as reports from human and nonhuman primate studies that different central pathways mediate histamine and nonhistamine itch (18–21). Because Nppb is critically required for pruriception in mice, future studies involving ablation and/or activation of the Nppb-expressing somatosensory neurons together with circuit tracing may reveal whether these cells directly trigger a spinal scratch reflex, are selective detectors for the sensation of itch, or are in fact more broadly tuned nociceptors. Such experiments will help reveal the central mechanism (or mechanisms) for itch, explain the interactions

between pruriception and other somatosensory signals, and ultimately provide a powerful stimulus for the rational design of novel therapies to alleviate chronic itch.

**References and Notes**

1. W. S. Shim *et al.*, *J. Neurosci.* **27**, 2331 (2007).
2. N. Imamachi *et al.*, *Proc. Natl. Acad. Sci. U.S.A.* **106**, 11330 (2009).
3. S. K. Han, V. Mancino, M. I. Simon, *Neuron* **52**, 691 (2006).
4. D. J. Cavanaugh *et al.*, *Proc. Natl. Acad. Sci. U.S.A.* **106**, 9075 (2009).
5. Y. G. Sun, Z. F. Chen, *Nature* **448**, 700 (2007).
6. Y. G. Sun *et al.*, *Science* **325**, 1531 (2009).
7. S. K. Mishra, S. M. Tisel, P. Orestes, S. K. Bhangoo, M. A. Hoon, *EMBO J.* **30**, 582 (2011).
8. Q. Liu *et al.*, *Cell* **139**, 1353 (2009).
9. Q. Liu *et al.*, *Sci. Signal.* **4**, ra45 (2011).
10. L. Han *et al.*, *Nat. Neurosci.* **16**, 174 (2013).
11. B. McNeil, X. Dong, *Neurosci. Bull.* **28**, 100 (2012).
12. K. S. Misono *et al.*, *FEBS J.* **278**, 1818 (2011).
13. M. J. Caterina *et al.*, *Science* **288**, 306 (2000).
14. R. G. Wiley, D. A. Lappi, *Adv. Drug Deliv. Rev.* **55**, 1043 (2003).
15. M. S. Fleming *et al.*, *Mol. Pain* **8**, 52 (2012).
16. M. Z. Li *et al.*, *Dev. Biol.* **292**, 555 (2006).
17. K. N. Patel, X. Dong, *Neuron* **68**, 334 (2010).
18. B. Namer *et al.*, *J. Neurophysiol.* **100**, 2062 (2008).
19. M. Schmelz, R. Schmidt, A. Bickel, H. O. Handwerker, H. E. Torebjörk, *J. Neurosci.* **17**, 8003 (1997).

20. L. M. Johaneck *et al.*, *J. Neurosci.* **28**, 7659 (2008).
21. S. Davidson *et al.*, *J. Neurophysiol.* **108**, 1711 (2012).

**Acknowledgments:** We are grateful to N. Ryba for encouragement and helpful advice and for valuable suggestions. The Nppb<sup>-/-</sup> mice used for this research project were generated from embryonic stem cells obtained from the National Center for Research Resources (NCRR)–NIH-supported KOMP repository ([www.komp.org](http://www.komp.org)) and engineered by the Wellcome Trust Sanger Institute and the Mouse Biology Program ([www.mousebiology.org](http://www.mousebiology.org)). We thank NIDCR Gene Targeting Facility for help generating Nppb mutant mice. The mouse strain STOCK Tg(GRP-EGFP) was obtained from the Mutant Mouse Regional Resource Center (MMRRC), a NCRR–NIH-funded strain repository, and was donated to the MMRRC by the National Institute of Neurological Disorders and Stroke-funded GENSAT BAC transgenic project. This research was supported by the intramural research program of the NIH, NIDCR.

**Supplementary Materials**

[www.sciencemag.org/cgi/content/full/340/6135/968/DC1](http://www.sciencemag.org/cgi/content/full/340/6135/968/DC1)  
Materials and Methods  
Figs. S1 to S4  
Tables S1 and S2  
References (22–25)  
Movies S1 to S3

7 December 2012; accepted 13 March 2013  
10.1126/science.1233765